Journal of Power Sources 189 (2009) 790–793

Contents lists available at ScienceDirect

Journal of Power Sources

journal homepage: www.elsevier.com/locate/jpowsour

Short communication

Structure studies on $LiMn_{0.25}Fe_{0.75}PO_4$ by in-situ synchrotron X-ray diffraction analysis

Yi-Chun Chen[a], Jin-Ming Chen[b], Chia-Haw Hsu[b], Jien-Wei Yeh[a], Han C. Shih[a,c,*], Yee-Shyi Chang[a], Hwo-Shuenn Sheu[d]

[a] Department of Materials Science and Engineering, National Tsing Hua University, Hsinchu 300, Taiwan
[b] Materials and Chemical Engineering, Industrial Technology Research Institute, Chutung 310, Taiwan
[c] Institute of Materials Science and Nanotechnology, Chinese Culture University, Taipei 111, Taiwan
[d] National Synchrotron Radiation Research Center, Hsinchu 300, Taiwan

ARTICLE INFO

Article history:
Received 19 June 2008
Accepted 24 July 2008
Available online 14 August 2008

Keywords:
LiMPO4
In-situ XRD
Phase transformation
Olivine structure

ABSTRACT

In this work, we substituted Mn^{2+} at the 4c site of $LiFePO_4$ to prepare $LiMn_{0.25}Fe_{0.75}PO_4$ in order to raise the working voltage. In order to study the phase transformation of lithium bi-metal phosphate ($LiM'M''PO_4$) during the lithiation/delithiation, in-situ synchrotron X-ray diffraction has been used. At 0.05*C* charge/discharge, X-ray patterns reveal that $LiMn_{0.25}Fe_{0.75}PO_4$ undergoes two two-phase transformations during the delithiation, resulting from Fe^{2+}/Fe^{3+} and then Mn^{2+}/Mn^{3+} redox reactions. However, the phase transformation for lithiation is different, becoming a two-phase (Mn^{2+}/Mn^{3+}) reaction and single-phase (Fe^{2+}/Fe^{3+}) reaction. Even at a higher charge/discharge rate (0.5*C*), the results are the same. $LiMn_{0.25}Fe_{0.75}PO_4$ also has a good cyclability, since there is no significant capacity fading during the cycling test. The X-ray patterns reveal that $LiMn_{0.25}Fe_{0.75}PO_4$ still maintains a good crystal structure after 40 cycles because of its stable olivine structure.

1. Introduction

Since the compound $LiFePO_4$ was used in rechargeable lithium ion batteries by Goodenough and co-workers [1], it has attracted a great deal of attention due to its low cost, safety and environmental friendliness [2–6]. $LiFePO_4$ has a stable olivine structure and a unique lithiation/delithiation mechanism. Lithium ions deintercalate from $LiFePO_4$, in association with the two-phase transformation ($LiFePO_4/FePO_4$). $LiFePO_4$ and $FePO_4$ both belong to the stable olivine structure, which makes $LiFePO_4$ very safe during the cell charge/discharge process. However, $LiFePO_4$ has a lower working voltage compared with other cathode materials, such as $LiCoO_2$, $LiCoNiO_2$ and $LiMnO_2$, due to the Fe^{2+}/Fe^{3+} system reaction at 3.4 V. Recently, many olivine-type cathode materials such as $LiMn_xFe_{1-x}PO_4$ and $LiCo_xFe_{1-x}PO_4$ have been studied in order to raise the working voltage [7,8], since the redox potentials of Mn^{2+}/Mn^{3+} and Co^{2+}/Co^{3+} are 4.1 V and 4.9 V, respectively.

Synchrotron X-ray diffraction is a powerful tool for studying the structure of materials because of its high energy continuous spectrum, excellent collimation, low emittance and high resolution. Consequently, synchrotron X-rays have been widely applied in the study of the structure of cathode materials for lithium ion batteries [9–12]. Chemical oxidation is a good way to accurately extract lithium ions from the cathode materials but this method cannot reveal the phase transformation and the lithiation together. In this work, we have prepared lithium bi-metal phosphate ($LiMn_{0.25}Fe_{0.75}PO_4$) as the cathode material. In-situ synchrotron X-ray analysis has been used to observe the real time phase transformations of $LiMn_{0.25}Fe_{0.75}PO_4$ during lithiation/delithiation.

2. Experimental

2.1. Powder preparation and cell fabrication

The compound $LiMn_{0.25}Fe_{0.75}PO_4$ was prepared by solid-state reaction between the compounds $FeC_2O_4{\cdot}2H_2O$, $MnCO_3$, $NH_4H_2PO_4$ and Li_2CO_3. Some glucose was added in order to enhance the conductivity and prevent the formation of Fe^{3+}. The precursors were dispersed into ethanol and ground by ball-milling. After evaporating the ethanol, the mixtures were first heated at 350 °C for 10 h in N_2 gas. The resulting $LiMn_{0.25}Fe_{0.75}PO_4$ was subsequently sintered at 700 °C for 10 h in a N_2 gas.

* Corresponding author at: Department of Materials Science and Engineering, National Tsing Hua University, Hsinchu 300, Taiwan. Tel.: +886 3 5715131 3845; fax: +886 3 5710290.
E-mail address: hcshih@mx.nthu.edu.tw (H.C. Shih).

0378-7753/$ – see front matter © 2008 Elsevier B.V. All rights reserved.
doi:10.1016/j.jpowsour.2008.07.088

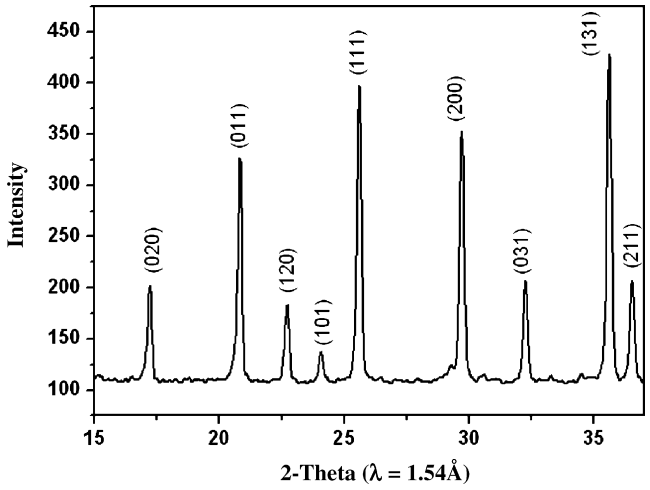

Fig. 1. The X-ray diffraction pattern of $LiMn_{0.25}Fe_{0.75}PO_4$.

For the in-situ X-ray experiment, the $LiMn_{0.25}Fe_{0.75}PO_4$ cathode was fabricated into an aluminum packaged film battery (4 cm × 2.5 cm × 1.5 mm) with a lithium metal anode. The cathode was constructed from $LiMn_{0.25}Fe_{0.75}PO_4$/carbon black/polyvinylidene fluoride with a weight ratio of 85/8/7 on the aluminum film. The cells were charged and discharged at 25 °C between fixed voltage limits (4.5–1.5 V) at constant current densities of 0.1 $mAcm^{-2}$ and 1 $mAcm^{-2}$ (approximating to the 0.05*C* and 0.5*C* rates) on an Arbin BT2400 battery tester. The structures were determined by X-ray diffraction (Siemens D6000Diffractometer).

2.2. In-situ XRD measurements

In-situ synchrotron X-ray studies were carried out in transmission mode at 16 keV (λ = 0.774 Å) at the Wiggler beam line 01*C* of the National Synchrotron Radiation Research Center, Hsinchu, Taiwan. The exposure time was 3 min and the XRD spectra were recorded on the Mar 345-image plate detector. All in-situ XRD patterns were calibrated using standard samples (Ag + Si) before further analysis.

3. Results and discussion

3.1. Structure analysis

Fig. 1 shows the X-ray diffraction pattern of the $LiMn_{0.25}Fe_{0.75}PO_4$ powders; all diffraction peaks can be indexed in the orthorhombic Pnma space group. The powders are solid solutions of $LiFePO_4$ and $LiMnPO_4$. The lattice parameters were calculated by the least squares method and gave a = 6.03 Å, b = 10.35 Å, c = 4.71 Å. In-situ XRD was then applied in order to study the phase transformation of $LiMn_{0.25}Fe_{0.75}PO_4$.

3.2. Electrical performance

Fig. 2 (a) and (b) shows the electrical performance (at 0.05*C* and 0.5*C*) of the $LiMn_{0.25}Fe_{0.75}PO_4$ electrode later used for the in-situ XRD experiments. In order to observe the phase transformation, the cell is operated at a low charge/discharge rate (0.05*C*) for the first cycle. There are two distinct plateaux, at 4 V and 3.5 V, from the Mn^{3+}/Mn^{2+} and Fe^{3+}/Fe^{2+} redox systems, respectively. The capacity is 153 mAh g^{-1} and the average working voltage rises to 3.53 V compared with 3.4 V for pure $LiFePO_4$. When the $LiMn_{0.25}Fe_{0.75}PO_4$ cell was used in the second cycle, at the 0.5*C*

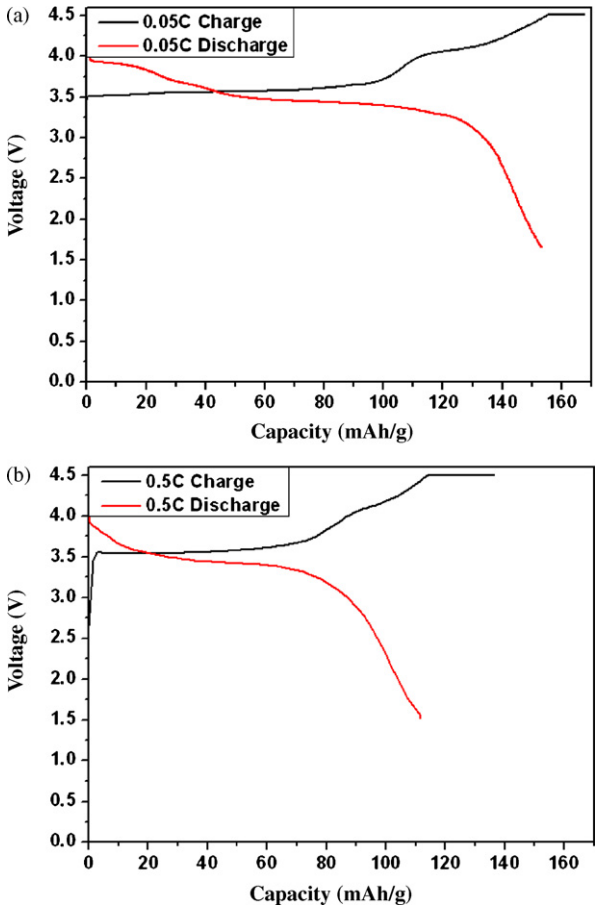

Fig. 2. The electrical performances of $LiMn_{0.25}Fe_{0.75}PO_4$ for in-situ XRD experiments (a) the first cycle 0.05*C* charge/discharge, (b) the second cycle 0.5*C* charge/discharge.

charge/discharge rate, the potential plateau of Mn^{3+}/Mn^{2+} became indistinct and the cell capacity decreased to 112 mAh g^{-1}, as shown in Fig. 2(b). Because olivine-type cathode materials have poor electrical conductivity, cells charged and discharged using a lower current density (<0.05*C*) may perform better and approach the theoretical capacity (170 mAh g^{-1}) [13].

3.3. In-situ X-ray diffraction analysis during the first cycle (0.05C charge/discharge)

Fig. 3 (a) shows the in-situ XRD patterns of $Li_xMn_{0.25}Fe_{0.75}PO_4$ as a function of the lithium content x during the cell charge at 0.05*C*. Before the cell charge (x = 1), the XRD pattern shows the $LiMn_{0.25}Fe_{0.75}PO_4$ electrode. Because the wave length is 0.774 Å, the $LiMn_{0.25}Fe_{0.75}PO_4$ (0 2 0) peak appears at 8.60°, shifted with respect to Fig. 1. During the delithiation, the in-situ XRD patterns confirm that $LiMn_{0.25}Fe_{0.75}PO_4$ undergoes two two-phase transformations. The first two-phase transformation is caused by the Fe^{2+}/Fe^{3+} redox reaction in $LiMn_{0.25}Fe_{0.75}PO_4$. At x = 0.62, the XRD pattern shows that the $Li_xMn_{0.25}{}^{2+}Fe_{0.75}{}^{3+}PO_4$ (0 2 0) peak begins to appear, indicating the coexistence of $Li_xMn_{0.25}{}^{2+}Fe_{0.75}{}^{2+}PO_4$ and $Li_xMn_{0.25}{}^{2+}Fe_{0.75}{}^{3+}PO_4$. The phase becomes entirely $Li_xMn_{0.25}{}^{2+}Fe_{0.75}{}^{3+}PO_4$ at x = 0.30 because the $Li_xMn_{0.25}{}^{2+}Fe_{0.75}{}^{2+}$ PO_4 (0 2 0) peak disappears in the XRD patterns. Afterwards there is a single-phase transformation between x = 0.30 and 0.23.

The second two-phase transformation is caused by the Mn^{2+}/Mn^{3+} redox reaction in $LiMn_{0.25}Fe_{0.75}PO_4$. The

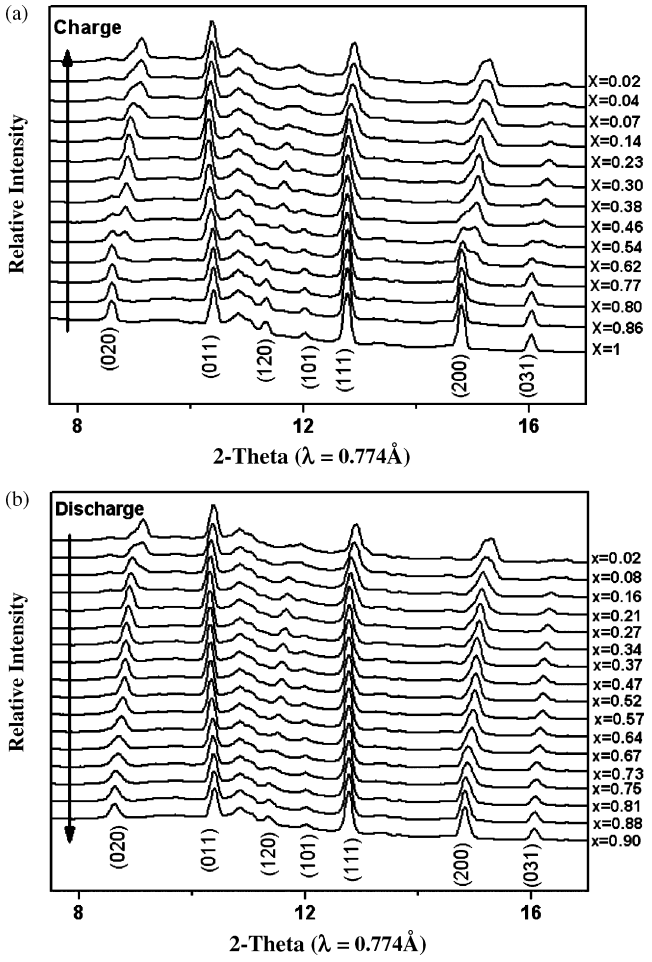

Fig. 3. In-situ XRD patterns of $Li_xMn_{0.25}Fe_{0.75}PO_4$ as a function of the lithium content x during the cell (a) charge and (b) discharge at 0.05*C*.

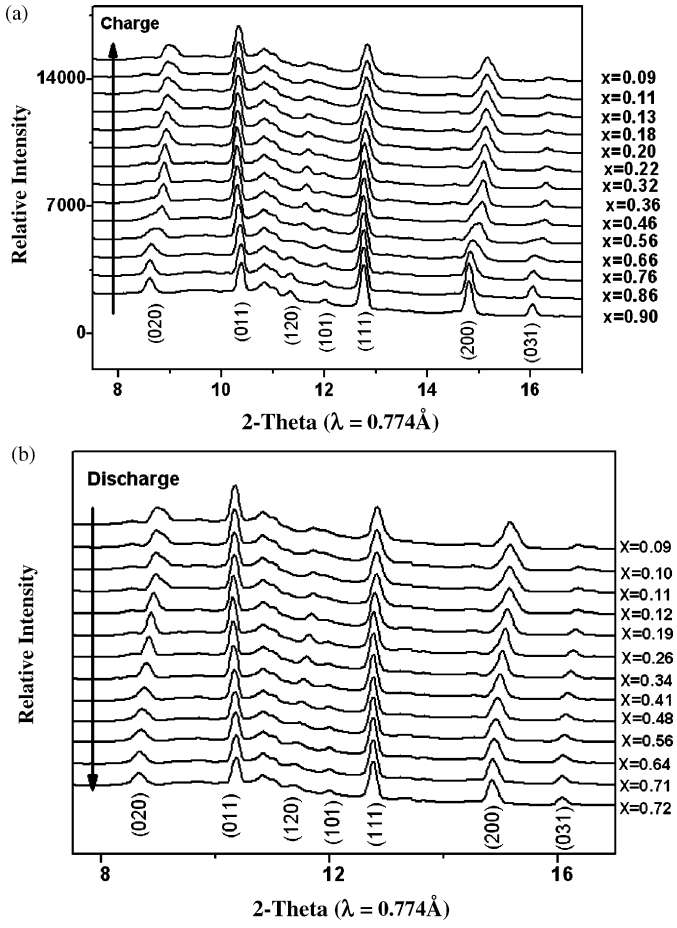

Fig. 4. In-situ XRD patterns of $Li_xMn_{0.25}Fe_{0.75}PO_4$ as a function of the lithium content x during the cell (a) charge and (b) discharge at 0.5*C*.

$Li_xMn_{0.25}{}^{3+}Fe_{0.75}{}^{3+}PO_4$ (0 2 0) peak begins to appear at $x = 0.14$ and the phase changes to $Li_xMn_{0.25}{}^{3+}Fe_{0.75}{}^{3+}PO_4$ at $x = 0.02$. The results are similar to those of Yamada et al. [14]. They used chemical oxidation to extract the lithium ion from $LiMn_xFe_{1-x}PO_4$ and constructed a phase diagram of $LiMn_xFe_{1-x}PO_4$ during the delithiation. But the one-phase region should be more limited in composition.

However, a different phase transformation is found during the lithiation, as shown in Fig. 3(b). $Mn_{0.25}Fe_{0.75}PO_4$ undergoes a two-phase and a single-phase transformation instead of two two-phase transformations. The two-phase transformation is caused by the Mn^{3+}/Mn^{2+} redox reaction ($Li_xMn_{0.25}{}^{3+}Fe_{0.75}{}^{3+}PO_4/Li_xMn_{0.25}{}^{2+}Fe_{0.75}{}^{3+}PO_4$) between $x = 0.02$ and 0.16. The two-phase transformation of Fe^{2+}/Fe^{3+} redox is not found in the lithiation process but is a single-phase reaction. The $Li_xMn_{0.25}Fe_{0.75}PO_4$ (0 2 0) peak shifts to the lower angle as the lithium ions intercalate, indicating that there is a solid solution of $Li_xMn_{0.25}{}^{2+}Fe_{0.75}{}^{3+}PO_4$ and $Li_xMn_{0.25}{}^{2+}Fe_{0.75}{}^{2+}PO_4$ in this region ($0.27 < x < 0.90$).

3.4. In-situ X-ray diffraction analysis of the second cycle (0.5C charge/discharge)

The XRD patterns show that $Li_xMn_{0.25}Fe_{0.75}PO_4$ also undergoes two two-phase transformations at the higher charge rate, as shown in Fig. 4 (a). The first two-phase transformation is the Fe^{2+}/Fe^{3+} redox reaction in $Li_xMn_{0.25}Fe_{0.75}PO_4$ and the second is the Mn^{2+}/Mn^{3+} redox reaction. The cell charge process ceases at $x = 0.09$, meaning that lithium ions cannot deintercalate completely from the $Li_xMn_{0.25}Fe_{0.75}PO_4$ structure at this higher charge rate because $LiMnPO_4$ has a poorer electrical conductivity than $LiFePO_4$ and a serious Jahn-Teller effect [15,16]. This result is also reflected by the XRD patterns. The phase is not transformed completely to $Li_xMn_{0.25}{}^{3+}Fe_{0.75}{}^{3+}PO_4$ when the cell charge process ends.

Fig. 4 (b) shows the in-situ XRD patterns of $Li_xMn_{0.25}Fe_{0.75}PO_4$ at the 0.5*C* discharge rate, which are consistent with the 0.05*C*

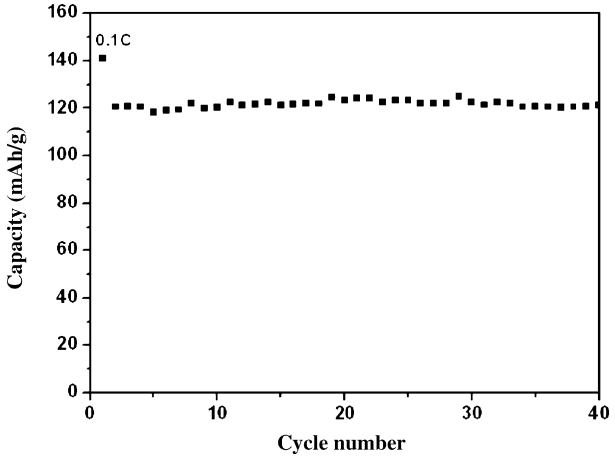

Fig. 5. The cyclic test of $LiMn_{0.25}Fe_{0.75}PO_4$ at 0.2*C* charge/discharge.

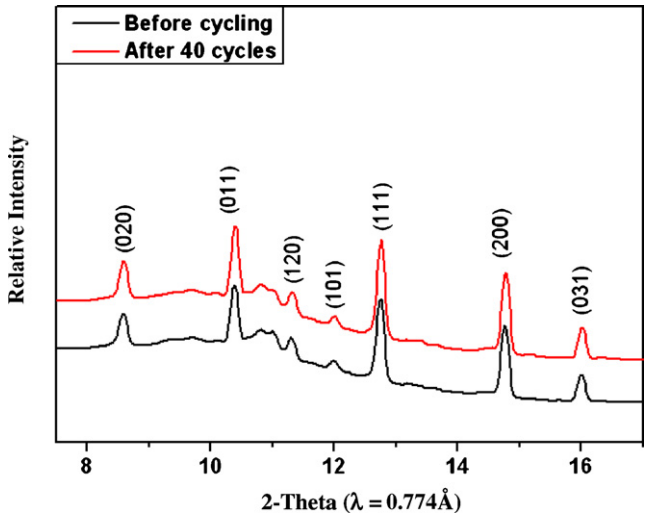

Fig. 6. Synchrotron XRD patterns of $LiMn_{0.25}Fe_{0.75}PO_4$ before (black line) and after (red line) cycling. (For interpretation of the references to colour in this figure legend, the reader is referred to the web version of the article.)

discharge rate. They show that $Li_xMn_{0.25}Fe_{0.75}PO_4$ follows the same phase transformations (two-phase and single-phase) even at the higher discharge rate.

3.5. Analysis of cyclic test

Fig. 5 shows the cyclic test of $LiMn_{0.25}Fe_{0.75}PO_4$ at the 0.2*C* charge/discharge rate. The capacity is about 120 mAh g^{-1} and there is no significant fading during the cycling, showing that it has good cyclability. Synchrotron X-ray diffraction was also used to study the relationship between the cyclability and structure. Fig. 6 shows the synchrotron XRD patterns of $LiMn_{0.25}Fe_{0.75}PO_4$ after cycling. Compared with a fresh electrode, the XRD patterns reveal that $LiMn_{0.25}Fe_{0.75}PO_4$ still maintains a good olivine structure after cycling, indicating that this cathode material has a stable structure and a good reversibility. This result is consistent with the cyclic test.

4. Conclusions

In this work, synchrotron X-ray diffraction has been applied to study the phase transformation of lithium bi-metal phosphate. Two significant two-phase transformations are observed by in-situ XRD during the delithiation. The first two-phase transformation is caused by the Fe^{2+}/Fe^{3+} redox reaction at 3.4 V and the other is the Mn^{2+}/Mn^{3+} redox reaction at 4.1 V. However, other phase transformations are found during the lithiation. The two-phase transformation of Mn^{3+}/Mn^{2+} redox is also found in the lithiation but only the single-phase transformation of the Fe^{3+}/Fe^{2+} redox. The $LiMn_{0.25}Fe_{0.75}PO_4$ retains good cyclability even after 40 cycles due to its stable olivine structure.

Acknowledgements

The authors gratefully acknowledge the support of this work by the National Science Council of the Republic of China under the contract of NSC95-2221-E007-042. We also thank J.J. Lee and W.T. Chuang for their technical assistance and the National Synchrotron Radiation Research Center (NSRRC) for use of their synchrotron X-ray diffraction facilities.

References

[1] A.K. Padhi, K.S. Nanjundaswamy, J.B. Goodenough, J. Electrochem. Soc. 144 (1997) 1188.
[2] S. Yang, Y. Song, P.Y. Zavalij, M.S. Whittingham, Electrochem. Commun. 4 (2002) 239.
[3] A. Yamada, S.C. Chung, K. Hinokuma, J. Electrochem. Soc. 148 (2001) A224.
[4] K. Zaghib, K. Striebel, A. Guerfi, J. Shim, M. Armand, M. Gauthier, Electrochim. Acta 50 (2004) 263.
[5] G.X. Wang, L. Yang, S.L. Bewlay, Y. Chen, H.K. Liu, J.H. Ahn, J. Power Sources 146 (2005) 521.
[6] K. Zaghib, P. Charest, A. Guerfi, J. Shim, M. Perrier, K. Striebel, J. Power Sources 146 (2005) 380.
[7] A. Yamada, S.C. Chung, J. Electrochem. Soc. 148 (2001) A960.
[8] D. Wang, Z. Wang, X. Huang, L. Chen, J. Power Sources 146 (2005) 580.
[9] X.Q. Yang, J. McBreen, W.S. Yoon, C.P. Grey, Electrochem. Commun. 4 (2002) 649.
[10] K.Y. Chung, W.S. Yoon, H.S. Lee, J. McBreen, X.Q. Yang, S.H. Oh, W.H. Ryu, J.L. Lee, W.I. Cho, B.W. Cho, J. Power Sources 163 (2006) 185.
[11] P.Y. Liao, J.D. Duh, J.F. Lee, H.S. Sheu, Electrochim. Electrochim. Acta 53 (2007) 1850.
[12] H.H. Chang, C.C. Chang, H.C. Wu, M.H. Yang, H.S. Sheu, N.L. Wu, Electrochem. Commun. 10 (2008) 335.
[13] H. Huang, S.C. Yin, L.F. Nazar, Electrochem. Solid-State Lett. 4 (2001) A170.
[14] A. Yamada, Y. Kudo, K.Y. Liu, J. Electrochim. Soc. 148 (2001) A1153.
[15] J. Chen, M.J. Vacchio, S. Wang, N. Chernova, P.Y. Zavalij, M.S. Whittingham, Solid State Ionics 178 (2008) 1676.
[16] J.N. Osorio-Guillen, B. Holm, R. Ahuja, B. Johansson, Solid State Ionics 167 (2004) 221.